Applied Surface Science 435 (2018) 149–155

Contents lists available at ScienceDirect

Applied Surface Science

journal homepage: www.elsevier.com/locate/apsusc

Full length article

Facile synthesis of Ag@ZIF-8 core-shell heterostructure nanowires for improved antibacterial activities

Yu-Feng Guo[a,b,1], Wei-Jun Fang[c,1], Jie-Ru Fu[a,b], Yun Wu[b], Jun Zheng[b,*], Gui-Qi Gao[b], Cheng Chen[b], Rui-Wen Yan[b], Shou-Guo Huang[a,*], Chun-Chang Wang[a,*]

[a] Laboratory of Dielectric Functional Materials, School of Physics and Material Science, Anhui University, Hefei, 230601, People's Republic of China
[b] Center of Modern Experimental Technology, Anhui University, Hefei, 230601, People's Republic of China
[c] College of Basic Medicine, Anhui Medical University, Hefei, 230032, People's Republic of China

ARTICLE INFO

Article history:
Received 22 July 2017
Received in revised form 11 October 2017
Accepted 12 November 2017
Available online 13 November 2017

Keywords:
Silver
ZIF-8
Core-shell heterostructure
Antibacterial activities

ABSTRACT

Compared with pure MOFs, core-shell heterostructures of noble-metal@MOFs have attracted tremendous interest due to their unique structure and extensive applications. In the present study, we have successfully synthesized well-defined core-shell Ag@ZIF-8 nanowires. The products growth process has been investigated by examining the products obtained at different intervals and the thickness of ZIF-8 shell ranging from 30 to 100 nm can be technically obtained by tuning the quantity of Ag nanowires. Ag@ZIF-8 has been proven to possess large specific surfaces and high thermal stability. Additionally, the antibacterial activity of Ag@ZIF-8 is further tested against *Bacillus subtilis* and *Escherichia coli* BL21. The results reveal that Ag@ZIF-8 core-shell heterostructure nanowires have effective activities against the two types of bacterial strains.

1. Introduction

Nowadays, core-shell heterostructures have attracted considerable attention owing to their improved performance compared with their single component, and these advantages make them one of the most promising candidates for the exploration of new applications in various fields [1–4]. Silver known as one of the most important noble metals has gained considerable interest for its applications in electronics, catalysis, lithium ion batteries and surface-enhanced Raman spectroscopy [5–8]. In addition, silver has been used extensively in many bactericidal applications due to its higher antimicrobial activities [9–14]. Among various nanostructures, nanowires have garnered particular attention owning to their superior properties in applications involving transparent conductor [15–17] and antimicrobial agents [18–20]. For example, Liu et al. fabricated Ag nanowires, which show good antibacterial activity [21]. However, nanostructured silver nanoparticles suffer from the shortcomings of easily aggregation and less stable, which apparently limit their antibacterial efficiency in practical applications [22–24]. Recently, Ag nanowires core-shell structures show excellent performances for practical applications [25–27]. For instance, Lee et al. reported a simple solution process synthesis of Ag-Au core-shell nanowire, which exhibited excellent electrical conductivity and stabilities [28]. Li and co-workers synthesized Ag@TiO_2 hierarchical core-shell nanowires, which exhibited good sustained antibacterial properties [29]. Hence, one rational strategy is to design core-shell heterostructures which could efficiently avoid the aggregation and improve the stability to enhance their antibacterial properties [30–33].

Porous metal-organic frameworks (MOFs) are attractive materials due to their promising field in catalysis, sensing, gas storage, imaging and antibacterium [34–38]. Meanwhile, compared with pure MOFs, noble-metal@MOFs core-shell heterostructure nanomaterials have become a booming research field owing to their cooperative behavior or multi-functionalities supplied by the combination of single component [39–43]. Herein, synthesis of the noble-metal@MOF core-shell heterostructure is the necessary prerequisite for improving their properties. However, few reports are concerned with construction of silver@MOF core-shell heterostructure [43,44], and their antibacterial activity has not been reported to date.

In this research, well-defined Ag@zeolitic imidazolate frameworks-8 (ZIF-8) core-shell heterostructure have been successfully synthesized. The Ag@ZIF-8 nanowires growth process has been investigated by examining the products obtained at

* Corresponding authors.
E-mail addresses: jzheng@ahu.edu.cn (J. Zheng), huangsg@ustc.edu (S.-G. Huang), ccwang@ahu.edu.cn (C.-C. Wang).
[1] These authors contributed equally to this work.

https://doi.org/10.1016/j.apsusc.2017.11.096
0169-4332/

different intervals and the thickness of ZIF-8 shell ranging from 30 to 100 nm can be technically obtained by tuning the quantity of Ag nanowires. Ag@ZIF-8 has been proven to possess large specific surfaces and high thermal stability. Importantly, antibacterial experimental results showed that the Ag@ZIF-8 core-shell heterostructure provide superior antibacterial activities against the two types of bacterial strains, displaying great potential as an effective antibacterial agent.

2. Experimental

2.1. Materials and methods

All the chemical reagents were purchased commercial suppliers and used as received without further purification. The Ag nanowires were prepared according to previous reported [45]. Typically, 0.15 g Polyvinylpyrrolidone (PVP) was added into 10 mL 1,2-propylene glycol and heated to 160 °C under vigorously stirring. After 1 h, 100 μL (10 mM in 1,2-propylene glycol) NaCl solution was injected into the flask with stirring. Subsequently, 4 mL $AgNO_3$ (0.15 M in 1,2-propylene glycol) was added under constant stirring. The solution was heated to 160 °C and stirred for 40 min. The precipitate were collected and washed with acetone and ethanol. In the second step, 6 mL as-prepared Ag nanowire (5 mg) was homogeneously dispersed in 25 mL ethanol by ultrasonication, and the mixture subsequently was placed in an ice bath. 0.0738 g 2-methylimidazole and 0.0248 g zinc acetate hexahydrate were added under magnetic stirring for 2 h. The samples were isolated by centrifugation and rinsed.

2.2. Characterization

X-ray diffraction (XRD) data was recorded in a PANalytical X'Pert diffractometer with Cu-Kα radiation. The size and morphology of the materials was investigated using a Hitachi S-4800 scanning electron microscopy (SEM) and a JEOL JEM-2100 transmission electron microscopy (TEM). A JEOL JEM-ARM200F was utilized to acquire the high-angle annular dark-field scanning TEM (HAADF-STEM) and energy-dispersive X-ray spectroscopy (EDS). The concentration of elemental Ag was analyzed using inductively coupled plasma-atomic emission spectrophotometer (ICP-AES, IRIS Intrepid II XSP). The thermogravimetric analyses (TGA) were characterized by a NETZSCH STA 449F3 under nitrogen atmosphere. Nitrogen adsorption-desorption isotherm were analyzed by a Micrometrics ASAP 2020 apparatus at 77 K.

2.3. Antimicrobial activity studies

Bacillus subtilis (Gram positive bacteria) and *Escherichia coli* BL21 (Gram negative bacteria) were assessed in all experiments. All the target bacteria were cultivated at 37 °C in LB (Luria-Bertani) broth until the bacteria concentration at approximately 10^9 colony forming units (CFUs) mL^{-1}. Then 100 μL of 10^9 CFU mL^{-1} bacterial suspensions were dispersed into 10 mL LB liquid medium containing different concentrations of Ag@ZIF-8 (0, 25, 50, 100, 200 and 300 μg mL^{-1}, respectively) and incubated at 37 °C. The growth rates were measured by monitoring the optical density (O.D.) at 600 nm. Parallel tests of Ag nanowires and ZIF-8 nanoparticles were also conducted for the comparison. The equation for quantitative antibacterial efficacy is given as follows [12]: $E(\%) = (1\text{-}B/A) \times 100\%$, where E(%) is the antibacterial efficacy, A represents the optical density value from the untreated bacteria suspension (without nanoparticles) and B is the optical density value from the bacteria suspension treated by the nanoparticles, respectively. The antibacterial properties of Ag@ZIF-8 on LB agar plates were also tested. 100 μL solution of Ag@ZIF-8 nanowires (0, 2.5, 5 and 10 mg mL^{-1}) was added onto the LB agar plates, and left to dry for 20 min at room temperature. Then, 100 μL of 10^3 CFU mL^{-1} bacterial suspensions were uniformly spread over the agar plates and subsequently incubated at 37 °C for 14 h.

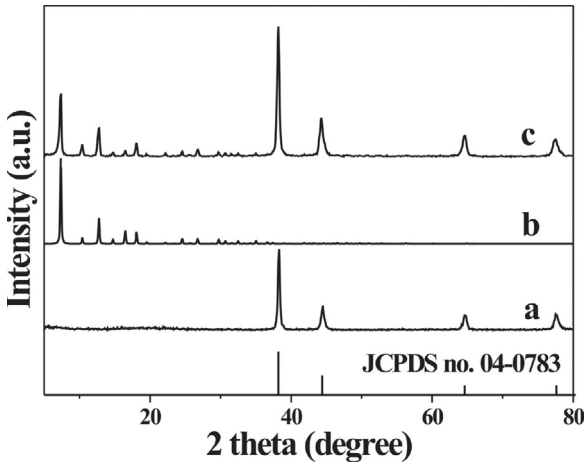

Fig. 1. Typical XRD patterns of Ag (curve a), simulated from ZIF-8 crystallographic data (curve b), Ag@ZIF-8 (curve c).

3. Results and discussion

As shown by curve a in Fig. 1, all the diffraction peaks are in good agreement with Ag (JCPDS no. 04-0783) before growth process. The apparent broadening of these peaks in width suggests that the as-synthesized Ag has smaller crystal sizes. From the XRD pattern, the Ag@ZIF-8 (curve c in Fig. 1) matches well with those of both Ag and ZIF-8 [46]. No additional diffraction peaks from possible impurities are observed, indicating the high purity of the as-synthesized Ag@ZIF-8.

SEM and TEM studies reveal the morphologies and detailed microstructures of the as-obtained products. Fig. 2a show panoramic SEM image of Ag nanowires with high purity and well-defined shapes. It can be clearly seen from Fig. 2b that the nanowires are uniform, with a size of about 70 nm in width and up to 2–3 μm in length. In the following procedure, the ZIF-8 nanoparticles are located on the outer layer of Ag nanowires to acquire the Ag@ZIF-8 heterostructure. Compared with the bare Ag nanowires as cores with relative smooth surfaces, the outside surface of the Ag@ZIF-8 becomes much rougher, as shown in Fig. 2c-d. With the ZIF-8 nanoparticles deposited, the Ag@ZIF-8 nanowires are up to 220 nm in width, whereas their lengths are little changed. Each Ag@ZIF-8 core-shell heterostructure possesses only one Ag nanowire core and ZIF-8 nanocrystals shell.

More structural information was further investigated by TEM. The low-magnification TEM image (Fig. 3a) demonstrates that the core-shell nanostructure is the primary morphology. As shown in Fig. 3b, it can be found that a clear contrast between the core and shell, and the thickness of core and shell are 75 nm and 70 nm, respectively. To further study the structural feature and distribution of elements of the Ag@ZIF-8, HAADF-STEM techniques were used. As shown HAADF-STEM images (Fig. 3c-d), the brightest nanowires are the Ag cores and each Ag nanowire was nicely encapsulated in ZIF-8 shell. The elemental mappings and EDX cross-sectional scans demonstrate that the distribution of Zn is bigger than that of Ag (Fig. 3e-g). The blue and purple lines represent Ag and Zn, respectively. The Ag content of the Ag@ZIF-8 was determined by ICP-AES, and the mass ratio of Ag to Ag@ZIF-8 is 40%. The above results unambiguously demonstrate that we have successfully prepared the Ag@ZIF-8 core-shell heterostructure.